2002

Experimental and theoretical study of benzene (acetonitrile)(n) clusters, n=1-4

M. Samy El-Shall
Virginia Commonwealth University

George M. Daly
Virginia Commonwealth University

Douglas Wright
Virginia Commonwealth University

El-Shall, M. S., Daly, G. M., Wright, D. Experimental and theoretical study of benzene (acetonitrile) n clusters, n=1–4. The Journal of Chemical Physics 116, 10253 (2002). Copyright © 2002 AIP Publishing LLC.

Experimental and theoretical study of benzene (acetonitrile)$_n$ clusters, $n=1-4$

M. Samy El-Shall,[a] George M. Daly,[b] and Douglas Wright
Department of Chemistry, Virginia Commonwealth University, Richmond, Virginia 23284-2006

(Received 9 January 2002; accepted 15 March 2002)

Well-resolved spectra of benzene–acetonitrile binary clusters BA_n, with $n=1-4$ have been obtained by the (one-color) resonant two-photon ionization technique using the benzene's $B_{2u} \leftarrow A_{1g}$ 0_0^0 and 6_0^1 resonances. The spectra reveal a rapid increase in complexity with the number of acetonitrile molecules in the cluster, associated with van der Waal modes and isomeric forms. While only single cluster origins are found for the benzene–acetonitrile (BA) and the BA_2 clusters, two and four distinct isomers are identified for the BA_3 and BA_4 clusters, respectively. The origins of the BA and BA_2 clusters are blueshifted with respect to the free benzene molecule by 38 cm^{-1} and 26 cm^{-1}, respectively. Monte Carlo (MC) simulations reveal two types of isomeric structures of the BA_n clusters. The clusters containing an even number of the acetonitrile molecules (BA_2, BA_4, and BA_6) are dominated by acetonitrile anti-parallel paired dimers. The BA_3 cluster consists of a cyclic acetonitrile trimer parallel to the benzene ring. In the BA_5 clusters, the acetonitrile molecules are assembled in a cyclic trimer + a paired dimer configuration or in two paired dimers + a single monomer structure. The R2PI spectra, in conjunction with the MC structural models and simple energetic arguments, provide a reasonably compelling picture of the spectroscopic and dynamical phenomena associated with dipole pairing molecular cluster systems. © *2002 American Institute of Physics.* [DOI: 10.1063/1.1476317]

I. INTRODUCTION

A molecular level understanding of the solvent effects in chemical reactions requires detailed knowledge of solute–solvent interactions including the size dependence of the spectral shifts and the evolution of intermolecular mode frequencies.[1–4] Gas phase molecular clusters provide models for such interactions since the size effect and the degree of complexity of the interaction potentials can be systematically varied in well-defined systems.[5–10] The influence of stepwise solvation on both the ground and the excited electronic states of a solute molecule can be probed by studying molecular clusters composed of a single ''solute'' molecule and selected numbers of ''solvent'' molecules. The solvent molecules can be chosen in such a way to present a wide range of intermolecular interactions which may result in small perturbations of the electronic states of the solute molecule or in large changes in the structure and electronic properties such as those associated with charge-transfer and excimer interactions. Such studies have been advanced by the development of powerful techniques, which enables one to isolate ultracold clusters containing a ''solute'' chromophore and selected numbers of ''solvent'' molecules. Among these techniques, resonant two-photon ionization (R2PI) has been extensively used as a selective spectroscopic tool for the study of molecular clusters of various sizes and compositions.[6–16,18–27]

Many cluster studies have utilized benzene as a prototypical aromatic solute chromophore for the study of a variety of solvent interactions with the conjugated π-system.[6,7,9,11–31] Its high symmetry reduces the complexity of the spectral assignments and the absence of a permanent dipole moment restricts the interactions with atoms or nonpolar molecules to exclusively dispersive forces. In benzene M_n clusters (BM_n), where M_n are heavy rare gas atoms, nonpolar or weakly polar molecules, a redshift has been observed in the electronic transition within the cluster relative to the same transition in the free benzene molecule.[6,7] In these systems, the spectral shifts originate essentially from dispersive and inductive interactions and the enhanced stabilization of the excited state has been rationalized in terms of increased polarization interaction between the excited benzene molecule and the solvent species.[6,32,33] On the other hand, in hydrogen bonding clusters, BS_n, where S is a hydrogen donor molecule such as H_2O,[23,24] CH_3OH,[26] $CHCl_3$,[22] HCl,[21] and CH_3COOH,[30] a blueshift has been observed thus indicating a decrease in the binding energy of the cluster upon the electronic excitation of benzene. These clusters have been the subject of systematic studies by Zwier's group and continue to attract much attention from both experimental and theoretical groups.[9,21–26,34–41] These studies have established several characteristic features for the clusters of benzene with hydrogen bonding molecules, which in turn have enhanced the current understanding of these systems.[9,34–41] Among these features are the blue spectral shifts in small clusters which seem to increase with increasing hydrogen bonding ability of the solvent molecules, the gradual switch to red shifts in larger clusters, the tendency of the solvent molecules to form a hydrogen bonding network in a one-sided structural type, and the very efficient fragmen-

[a]Author to whom correspondence should be addressed.
[b]Present address: Purdue Pharma L.P., Ardsley, New York 10502.

tation of the photoionized clusters which has been interpreted as a direct consequence of the hydrogen bonding to the benzene ring.[9] It is not clear, however, if these features are unique to hydrogen bonding clusters or are probably to be expected for most clusters where the interactions among the solvent molecules are dominated by electrostatic forces. For a full understanding of these systems, it is therefore desirable to study clusters of benzene with highly polar solvent molecules that are not capable of forming a hydrogen-bonding network.

The particular system of interest in the present study, consists of a single benzene molecule (B) interacting with acetonitrile molecules, A_n i.e., BA_n with $n=1-4$. In contrast to water, acetonitrile is unable to participate in relatively strong hydrogen bonding to the π-system of benzene since the hydrogen bonding interactions via the methyl group are very weak. However, the presence of the cyano group with its electron withdrawing ability is expected to activate the methyl hydrogens for specific interactions with the benzene ring.[42] Acetonitrile clusters have already been the subject of both experimental and theoretical studies.[43–53] Because of the large dipole moment of acetonitrile (3.9 D), the interactions within these clusters are dominated essentially by dipole–dipole forces, and the lowest energy structures reflect the favorable antiparallel pairing of the molecular dipoles. Molecular dynamics (MD) and Monte Carlo (MC) studies have shown that the antiparallel pairing of the dipoles may lead to rigid solidlike structures of the *n*-even clusters with melting transition temperatures considerably higher than those of the *n*-odd clusters.[50,51] Acetonitrile clusters containing a benzene molecule raise the interesting question of whether the structural features observed in the neat clusters would be retained in the presence of benzene, and whether the spectral shifts of BA_n clusters would provide any evidence for the dipole pairing and the associated even/odd character observed in the neat clusters. If the dipole–dipole interaction between the acetonitrile molecules is stronger than the dipole-induced dipole interaction between acetonitrile and benzene, then little changes are to be expected in the gross structural feature of the clusters when benzene chromophore is placed within the acetonitrile clusters. The examination of this and other related questions is the subject of the present work, which presents the results of ultraviolet spectroscopy of the BA_n clusters for $n=1-4$. In addition, we examine the structural properties of the BA_n clusters with $n=1-6$ using MC simulations. The combination of the experimental results and structural investigations provides sufficient information to establish some novel conclusions on these clusters.

II. EXPERIMENT

Binary benzene–acetonitrile clusters are generated by pulsed adiabatic expansion in a supersonic cluster beam apparatus.[30,31,54,55] The essential elements of the apparatus are jet and beam chambers coupled to a time-of-flight mass spectrometer. The binary clusters are formed in a He-seeded jet expansion, and probed as a skimmed cluster beam in a collision-free high vacuum chamber with a delay between synthesis and probe (i.e., the neutral beam flight time) on the order of one millisecond. During operation, a vapor mixture of benzene and acetonitrile (Aldrich, 99.9% purity), in He (ultrahigh purity, Spectra Gases 99.999%) at a pressure of 2–8 atm is expanded through a conical nozzle (100 μm diam) in pulses of 200–300 μs duration at repetition rates of 8–10 Hz. The composition of the benzene–acetonitrile vapor mixture is controlled by bubbling He through two separate, temperature controlled glass bubblers containing samples of benzene and acetonitrile. It is found in repeated experiments that cold BA_n clusters can be generated with minimum contributions of $(benzene)_2$-containing clusters in the beam by using a benzene–acetonitrile vapor mixture of approximately 1:10 ratio, which in turn is mixed in He at a total pressure of 7 atm, thus giving benzene/acetonitrile/He seed ratios of approximately 1:10:500. The jet is skimmed and passed into a high vacuum chamber, which is maintained at 8×10^{-8}–2×10^{-7} Torr. The collimated cluster beam passes into the ionization region of the TOF mass spectrometer where it intersects a laser pulse from a frequency-doubled dye laser. The tunable radiation is provided by a dye laser (Lambda Physik FL3002) pumped by an excimer laser (Lambda Physik LPX-101). Coumarin 500 (Exciton) dye laser output passes through a β-BaB_2O_4 crystal (CSK Co.) to generate a continuously tunable frequency-doubled output of 10^{-8} s pulses. The spatially filtered (using a set of four quartz Pellin–Broca prisms) ultraviolet radiation is adjusted to minimize three photon processes while still providing sufficient ion current (photon power density $\approx10^6$ W/cm^2). The laser system has $\approx$0.10 cm^{-1} bandwidth at 40 000 cm^{-1} (250 nm). The cluster ions formed by the R2PI are electrostatically accelerated in a two-stage acceleration region (300–400 V/cm), and then travel a field-free region (140 cm in length) to a two-stage microchannel-plate detector. Deflection plates are used to compensate for the cluster beam velocity. The TOF spectrum is recorded by digitizing the amplified current output of the detector with a 500 MHz digitizer (LeCroy 9350A) and averaged over 200 pulses. In addition to R2PI, the BA_n cluster beam is detected coaxially by a quadrupole mass spectrometer (Extrel C-50) with an EI source, which is used to characterize the overall composition

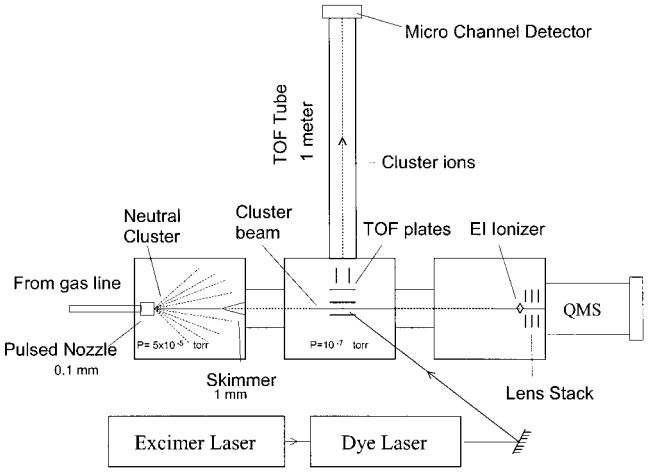

FIG. 1. Experimental setup for the cluster beam time-of-flight and quadrupole mass spectrometers.

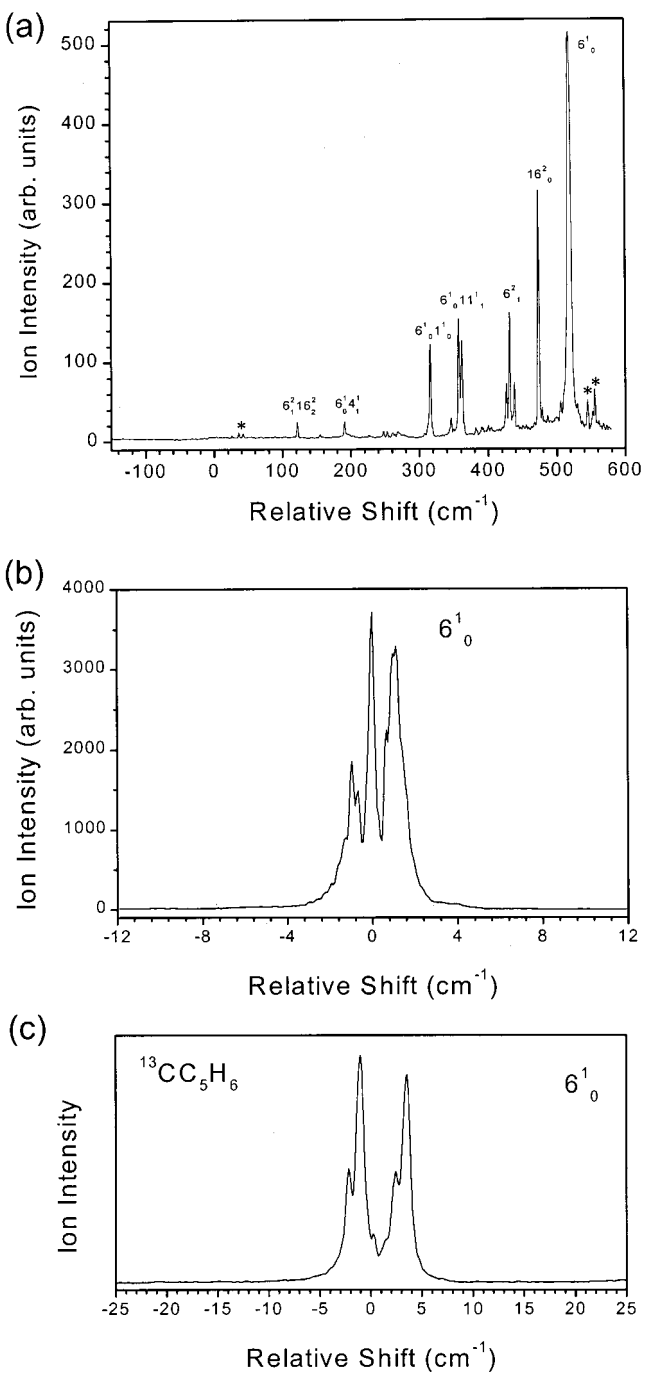

FIG. 2. (a) One-color R2PI spectrum of benzene (C_6H_6) in the region of the $^1B_{2u} \leftarrow {}^1A_{1g}$ transition. (b) High resolution of the 6^1_0 band of C_6H_6, $m/z=78$. (c) Splitting of the 6^1_0 band in $^{13}CC_5H_6$ (one ^{13}C isotope in C_6H_6, $m/z=79$).

of the beam, including such species as acetonitrile clusters (A_n), which are transparent in the laser spectroscopy experiments. The use of the quadrupole mass spectrometer in the current investigation has proven useful in quantitatively optimizing the cluster beam conditions for the species of interest in the spectroscopic experiments. Figure 1 illustrates the experimental setup with the two mass spectrometers used in these experiments.

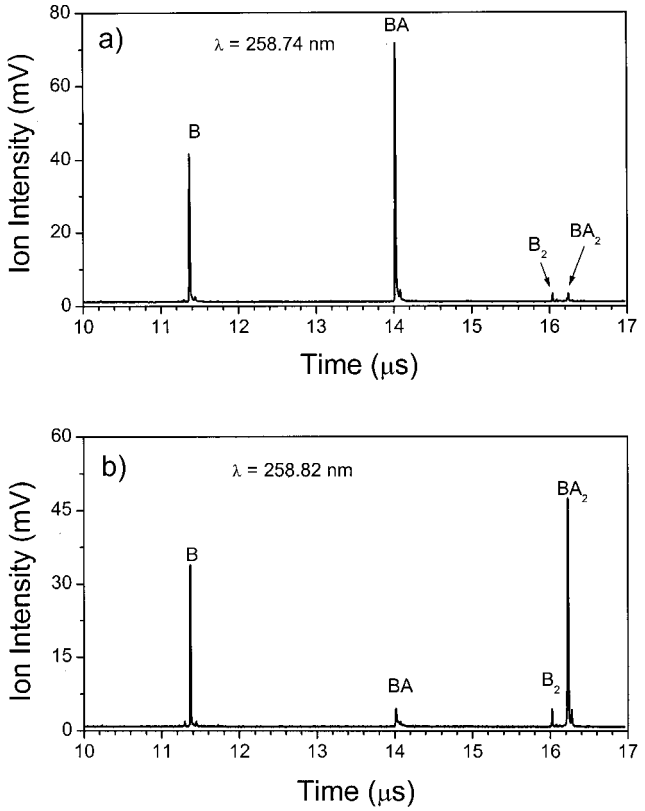

FIG. 3. R2PI mass spectra of the benzene–acetonitrile (BA) cluster beam obtained at the resonance excitations assigned to the origins of BA and BA_2 clusters at (a) 258.74 nm and (b) 258.82 nm, respectively.

III. COMPUTATIONAL DETAILS

Cluster interaction energies were calculated from site–site potentials of the form,

$$\Delta\varepsilon_{ab}=\sum_i^{on\ a}\sum_j^{on\ b}\left(\frac{q_iq_je^2}{r_{ij}}+\frac{A_{ij}}{r_{ij}^{12}}-\frac{C_{ij}}{r_{ij}^{6}}\right),$$

where $\Delta\varepsilon_{ab}$ is the interaction energy between two molecules a and b, and the A_{ij} and C_{ij} can be expressed in terms of Lennard-Jones σ's and ε's as $A_{ii}=4\varepsilon_i\sigma_i^{12}$ and $C_{ii}=4\varepsilon_i\sigma_i^6$ and the combining rules[56] $A_{ij}=(A_{ii}A_{jj})^{1/2}$ and $C_{ij}=(C_{ii}C_{jj})^{1/2}$ were used. The q_i are the partial charges assigned to each site and e is the magnitude of the electron charge. This form was used for all site–site interactions, between like and unlike molecules. The potential parameters and molecular geometry for benzene were taken from Jorgensen *et al.*[57] (OPLS 12-site potential), and for acetonitrile these were taken from Bohm *et al.*[58] (six-site model). The starting structures were obtained by beginning from the minima for the pure acetonitrile clusters obtained in our previous study,[49] and then allowing a benzene molecule to condense onto the "cluster surface" at $T=10^{-6}$ K. Each cluster was gradually warmed from this initial configuration.

Minima on the potential surface were located by the following procedure. Beginning from a lattice fragment or a previous minimum, the cluster was expanded by scaling the coordinates and giving each molecule a rather large random

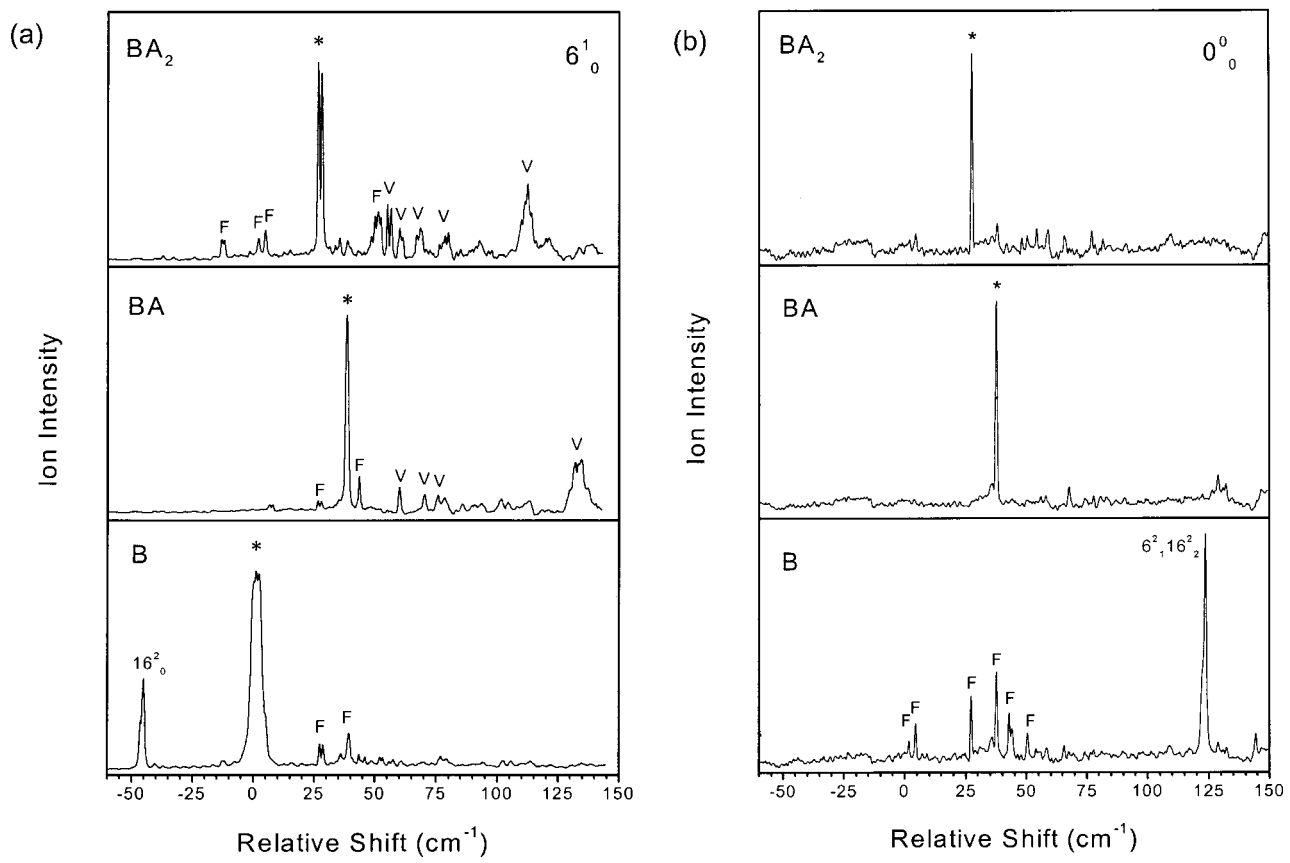

FIG. 4. One-color R2PI spectra measured in the benzene (B), benzene [acetonitrile] (BA) and benzene [acetonitrile]$_2$ (BA_2) mass channels relative to (a) the 6_0^1 and (b) the 0_0^0 transitions of benzene.

displacement (up to 5 Å) and rotation (up to 180°). The resulting random configuration was then allowed to relax into minima by making the usual small random displacements and rotations and allowing only new configurations that are lower in energy than the preceding configuration.[59] Eventually a minimum will be reached, and when 6000–15000 consecutive trial configurations fail to find a structure of lower energy, the configuration is identified as a candidate for a minimum on the surface. Subsequently, in a separate calculation, each candidate is run at 10^{-6} K to confirm that a minimum has in fact been located (the energy and intermolecular distances were stable) and to be sure that the bottom of the well has been reached. If there was any downward drift in the energy, the cluster was run at 10^{-6} K until there was no further drift to six decimal places. For each cluster composition, BA_n, typically 200–400 ''quenches'' from random configurations were performed. Most individual minima were located numerous times, although the calculation method does not allow statistical data to be extracted from the minima frequencies for a cluster of given composition.

IV. RESULTS AND DISCUSSION

A. The benzene mass channel

The two resonance excitations used in the present experiments are 6_0^1 and the 0_0^0 transitions of benzene.[60] Figure 2(a) exhibits the R2PI spectra of benzene in the region of the $^1B_{2u} \leftarrow {}^1A_{1g}$ transition obtained by monitoring the mass channel corresponding to benzene (C_6H_6). The spectrum is presented in relative frequency with respect to the forbidden origin. The strongest feature in the spectrum corresponds to the 6_0^1 transition at 523 cm^{-1}.[57] The other major features of the spectrum are due to hot bands as well as excitations to overtone and combination bands. In addition, three minor features (marked with asterisks) correspond to BA_n clusters that fragment to the benzene mass channel. These features will be discussed in the next section.

Figure 2(b) displays the benzene 6_0^1 band under high resolution where the *P*, *Q*, and *R* branches are clearly visible, and the center position of the multiplet (*Q* branch) is assigned to the origin of the 6_0^1 band (38 611 cm^{-1}). Starting from the benzene's vibronic ground state (A_{1g} symmetry), transitions in this region are to states of vibronic symmetry E_{1u}. In principle, an asymmetrical distribution of atoms about the C_6 axis would lift this degeneracy, producing a small splitting of the transition.[57] This is clearly seen in Fig. 2(c) which exhibits the R2PI spectrum of benzene obtained by monitoring the channel corresponding to $^{13}CC_5H_6$ (one ^{13}C isotope in C_6H_6, $m/z=79$). The spectrum shows that the replacement of a ^{12}C with a ^{13}C in the benzene ring results in sufficient lowering of the symmetry to remove the degeneracy of the 6_0^1 band, causing a splitting of 2.5 cm^{-1}, in excellent agreement with the spectrum reported by Bosel.[61] Similarly, the 6_0^1 splitting can also be produced by an asym-

TABLE I. Spectral features observed in the BA and BA_2 mass channels ($m/z=119$ and 160 amu, respectively). B=benzene, A=acetonitrile, F=fragment, vdw=van der Waals mode.

Shift (cm^{-1}) from the 6_0^1 of benzene	Assignment	Relative intensity	Shift (cm^{-1}) from the cluster's origin
	BA		
25.9	F (BA_2)	5.7	
27.2	F (BA_2)	5.3	
37.2	BA origin	100.0	0
42.9	F (B_2A)	8.2	
59.2	vdw	6.0	21.6
69.4	vdw	4.6	31.8
75.0	vdw	4.5	37.4
77.6	vdw	4.0	40.0
131.1	vdw	10.9	93.5
132.3	vdw	10.7	94.7
133.5	vdw	11.5	95.9
	BA_2		
−13.7	F (BA_3)	10.0	···
−12.7	F (BA_3)	9.7	···
1.3	F (BA_3)	10.7	···
4.1	F (BA_3)	14.8	···
25.9/27.2	BA_2 origin	100/95	
47.7	vdw	5.9	21.2
49.0	vdw	9.8	22.5
50.3	F (BA_4)	10.7	
51.4	F (BA_4)	9.6	
54.1	vdw	12.2	27.6
55.6	vdw	11.6	29.1
59.1	vdw	7.4	32.3
60.4	vdw	5.6	33.9
66.0	vdw	6.2	39.5
67.5	vdw	7.6	41.0
77.4	vdw	6.0	50.9
78.9	vdw	6.5	52.4
110.1	vdw	12.8	83.6
111.2	vdw	16.2	84.7
112.7	vdw	10.6	86.2
114.6	vdw	5.0	88.1

metrical distribution of clustering atoms or molecules around the C_6 axis of benzene as will be shown below.

B. Spectra of $n=1$ and 2 clusters

Figure 3 exhibits the mass spectra of the cluster beam obtained at two different wavelengths for a typical expansion of benzene:acetonitrile:He mixture with a relative concentration ratio of 5:16:1000, respectively. At 258.74 nm, the 1:1 complex (BA) is the most abundant ion observed while at 258.82 nm the BA_2 ion becomes the most abundant. This is a direct result of the resonance ionization where the neutral clusters are selectively ionized via their distinct resonance transitions. The significant intensity of the benzene ion is a result of van der Waals (vdW) fragmentation from larger BA_n and B_n clusters.

Figure 4(a) presents the R2PI spectra obtained by monitoring the mass channels corresponding to B^+, B^+A, and B^+A_2 in the 6_0^1 region of the benzene monomer between 38 550 and 38 750 cm^{-1}. The BA channel shows a single intense peak blue shifted relative to the 6_0^1 transition of the benzene by 37.6 cm^{-1}. The B^+A_2 channel exhibits a doublet at 25.9/27.2 cm^{-1} also to the blue of the benzene 6_0^1 band. These features are identified as the 6_0^1 resonances of the BA and BA_2 clusters, respectively.[62] The effects of fast (submicrosecond) ion fragmentation are clearly evident in Fig. 4(a), where the features associated with BA_2 and BA clusters also appear in the lower channels of B^+A and B^+, respectively. Furthermore, the doublet peak assigned to the BA_2 cluster appears in the B channel with more intensity than in the B^+A channel. This suggests that the $n^+ \rightarrow (n-2)^+$ fragmentation process in the B^+A_2 cluster is more efficient than the usual $n^+ \rightarrow (n-1)^+$ process typically observed in the one-color R2PI experiments.

The R2PI spectra in the 0_0^0 region of the benzene monomer obtained by monitoring the mass channels of the B^+A and B^+A_2 clusters are shown in Fig. 4(b). The spectra are very similar to the 6_0^1 spectra displayed in Fig. 4(a). The features assigned to the 6_0^1 resonances of the BA and BA_2 clusters are readily observed in the 0_0^0 region at $+37$ cm^{-1} and $+24$ cm^{-1} relative to the benzene forbidden 0_0^0 band. The observed intensity ratios of the 0_0^0 to the 6_0^1 absorption bands of the BA and BA_2 clusters are 0.08 and 0.10, respectively. In calculating these ratios, contributions from more than one mass channel are added in cases where the resonant features appear in the lower mass channels as a result of fast ion fragmentation.

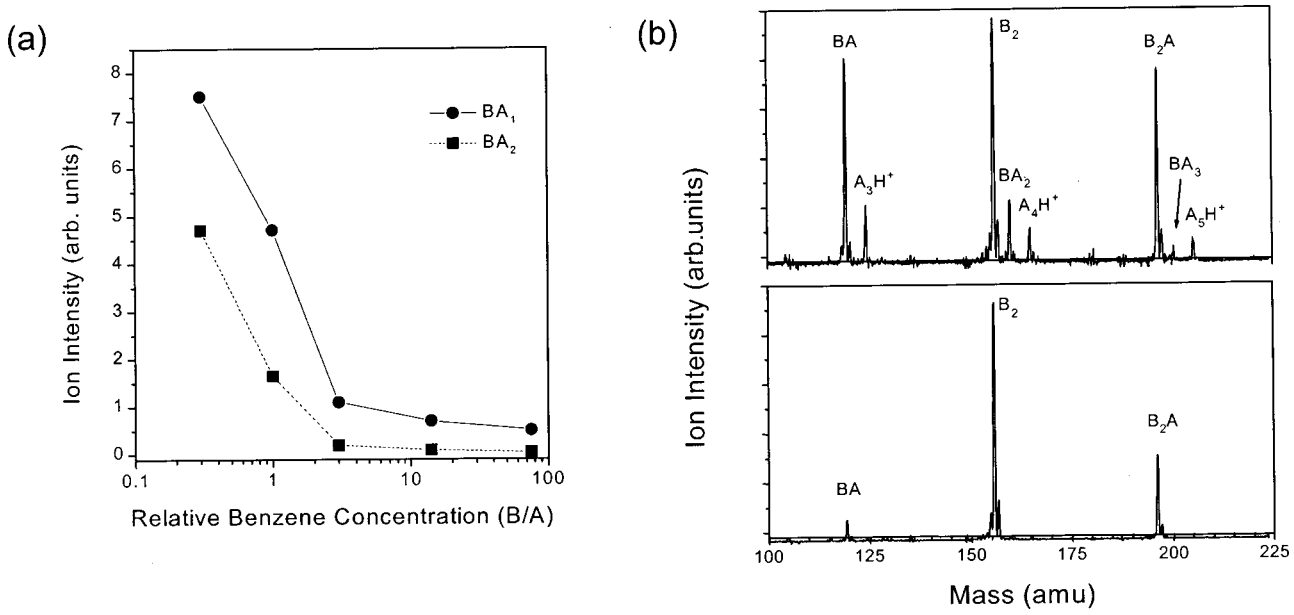

FIG. 5. (a) The dependence of the ion intensity assigned to the BA and BA_2 clusters on the benzene/acetonitrile pressure ratio in the pre-expansion mixture. (b) Electron impact mass spectra of the benzene–acetonitrile (BA) cluster beam obtained with B:A pressure ratio in the pre-expansion mixture of 1:1 (top) and 75:1 (bottom).

Comparing the 6_0^1 and the 0_0^0 features, it is noticeable that the BA_2 band that is clearly split in the 6_0^1 shows no splitting in the 0_0^0 transition. Also, in both cases, several weaker features appear on the blue side of the origin and are assigned to the excitation of the intermolecular vdW of the clusters. Among these features are four relatively strong bands [labeled v in Fig. 4(a)] centered around 59, 69, 78, and 132 cm^{-1} for BA and 55, 60, 67, and 112 cm^{-1} for BA_2 (relative to the 6_0^1 band of benzene). The relative frequencies and tentative assignments of the BA and BA_2 features are listed in Table I.

To examine the dependence of the R2PI spectra on the composition of the cluster beam we measured the relative intensity of the 6_0^1 bands assigned to the BA_2 and BA as a function of the relative concentration of benzene: acetonitrile in the pre-expansion vapor mixture. The results, displayed in Fig. 5(a), show that the intensities of B^+A and B^+A_2 decrease monotonically as the concentration of acetonitrile relative to that of benzene decreases in the pre-expansion mixture. Furthermore, as the B^+A_2 intensity decreases no new features appear in either the BA or the B channel, which could be assigned, to the BA complex. This is evident in Fig. 5(b) which shows the cluster ion distribution obtained by EI ionization at two different beam compositions with B:A pressure ratios of 1:1 and 75:1. It is clear that the beam generated from the expansion of a vapor mixture containing 75:1 mole ratio of B:A contains negligible concentration of the BA_2 species. This provides further evidence that the R2PI spectra obtained from the same beam by monitoring the B^+A channel must be due to the BA complex and not as a result of ion fragmentation from higher clusters. The consistency between the EI and the TOF results indicates that the ion distributions observed are qualitatively related to the concentrations of the neutral clusters in the beam.

It is also important to note that at a very low concentration of acetonitrile in the pre-expansion mixture, the cluster beam is dominated with benzene clusters (B_n) and benzene clusters containing a single acetonitrile molecule (B_nA). The R2PI features of these clusters (B_nA) are redshifted relative to the free benzene molecule and therefore they present no interference problem that could arise from the fragmentation process $B_2^+A \rightarrow B^+A$. The spectroscopy of the B_nA series in comparison with pure benzene clusters has been presented and discussed in a recent report.[31]

The assignment of the 37.6 cm^{-1} band to the origin of the BA complex is consistent with the results of the 1-cyanonapthalene (1-CNN)–acetonitrile complex.[63] The fluorescence excitation spectra of the complex revealed the existence of two isomers associated with the spectral features at -175 and 39 cm^{-1} relative to the 0_0^0 transition of 1-CNN at 31 400 cm^{-1}. The redshifted apectrum was assigned to the antiparallel arrangement of the dipoles of the cyano groups in 1-CNN and acetonitrile. This dipole–dipole interaction is expected to be larger in the excited state. The blueshifted spectrum was assigned to a conformation involving preferential interaction of acetonitrile methyl group with the unsubstituted ring of 1-CNN.[64] This structure is very similar to the benzene–acetonitrile structure and therefore, the blueshift of 37.6 cm^{-1} with respect to the aromatic chromophore is observed in both cases.

C. Spectra of $n=3$ and 4 clusters

The R2PI spectra obtained by monitoring the mass channel corresponding to the B^+A_3 cluster in the regions of the benzene 6_0^1 and 0_0^0 transitions are displayed in Fig. 6(a). These spectra are far more complicated than the spectra of the $n=1$ and 2 complexes partially because of the appearance of several new features which could either be assigned to conformational isomers or to vdW intermolecular modes.

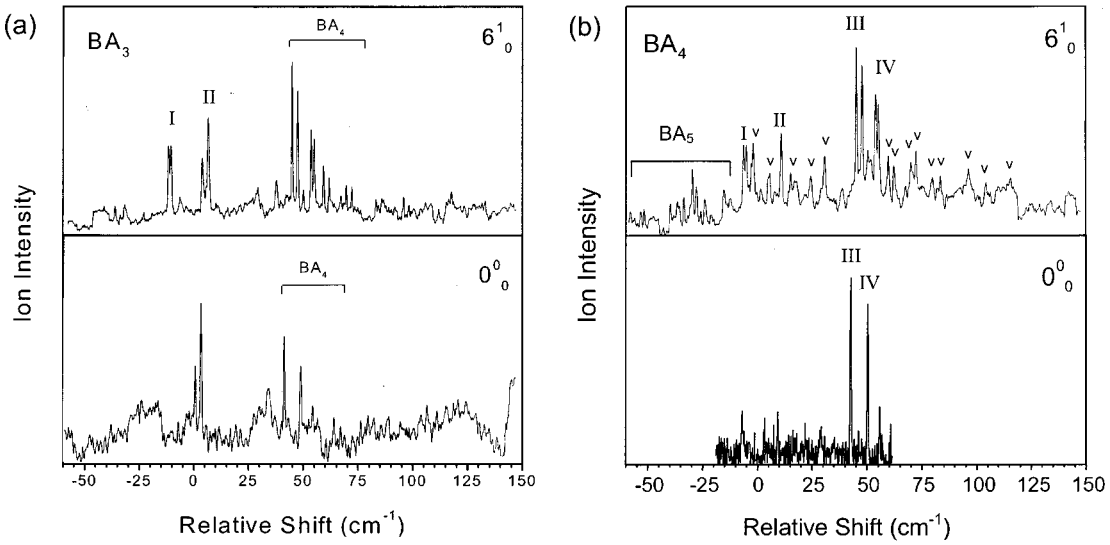

FIG. 6. One-color R2PI spectra measured in (a) the BA_3 and (b) the BA_4 mass channels relative to the 6_0^1 and the 0_0^0 transitions of benzene.

TABLE II. Spectral features observed in the BA_3 and BA_4 mass channels ($m/z=201$ and 242 amu, respectively), B=benzene, A=acetonitrile, F=fragment, vdw=van der Waals mode.

Shift (cm^{-1}) from the 6_0^1 of benzene	Assignment	Relative intensity
	BA_3	
−13.8/−12.6	Origin BA_3 isomer I	60/58
1.4/4.1	Origin BA_3 isomer II	52/100
41.8	F (BA_4)	142
44.4	F (BA_4)	120
46.9	F (BA_4)	35
50.3	F (BA_4)	84
51.7	F (BA_4)	71
55.9	F (BA_4)	40
58.4	F (BA_4)	36
65.9	F (BA_4)	32
68.5	F (BA_4)	36
79.3	F (BA_4)	21
91.8	F (BA_4)	28
99.5	F (BA_4)	21
	BA_4	
−31.8	F (BA_5)	31
−8.6/−7.5	Origin BA_4 isomer I	45
−5.1	vdw isomer I	34
−4.3	vdw isomer I	46
2.9	vdw isomer I	29
8.2	Origin BA_4 isomer II	52
12.3	vdw isomer II	29
21.5	vdw isomer II	27
27.8	vdw isomer II	39
41.8/44.4	Origin BA_4 isomer III	100/90
50.4/51.7	Origin BA_4 isomer IV	73/68
55.9	vdw isomer III	39
58.4	vdw isomer III	33
65.9	vdw isomer IV	35
68.4	vdw isomer IV	41
79.4	vdw isomer IV	27
91.8	vdw isomer IV	32
99.5	vdw isomer III	24
110.9	vdw isomer III	26

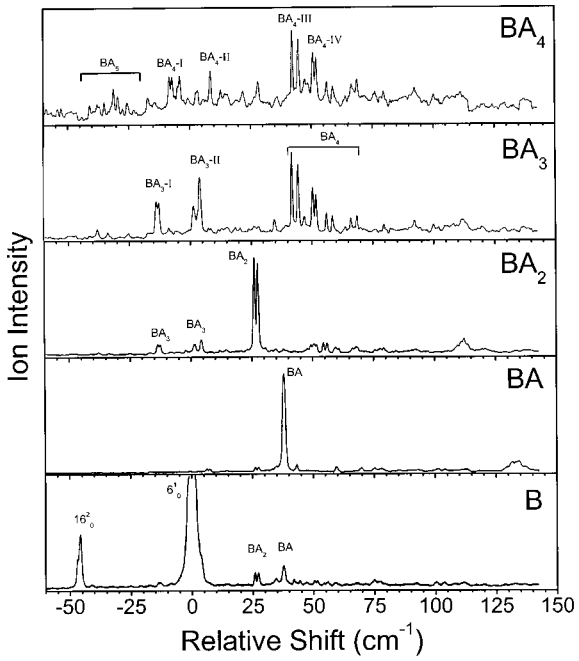

FIG. 7. One-color R2PI spectra measured in the BA_n mass channels with $n=1-4$, relative to the 6_0^1 transition of benzene.

In addition, ion fragmentation appears to be more pronounced in the $n=3-5$ clusters. For example, the features appearing in the B^+A_3 channel are due to both the BA_3 and BA_4 clusters. In the 6_0^1 spectrum the most intense low energy feature is assigned to the 6_0^1 vibronic origin of one geometrical isomer of the BA_3 cluster (isomer BA_3-I). This feature exhibits a small splitting of about 1.2 cm^{-1}thus giving rise to a doublet at -12.6 and -13.8 cm^{-1} from the benzene 6_0^1 band. Another strong doublet appears at 1.4 and 4.2 cm^{-1} to the blue of the 6_0^1 of benzene and is assigned to a second isomer of the BA_3 cluster (isomer BA_3-II).

The 6_0^1 origin of the BA_3-I isomer ($-12.6/-13.8$ cm^{-1}) appears with very weak intensity in the 0_0^0 spectrum. The small splitting observed in the 6_0^1 transition (~ 1 cm^{-1}) does not appear in the 0_0^0 spectrum and the ratio of $0_0^0/6_0^1$ is only 2%. The situation is completely different for isomer II where the two features at $+1.4$ and 4.2 cm^{-1} are clearly observed in the 0_0^0 spectrum with an average intensity ratio of more than 8% relative to the 6_0^1 spectrum.

The 6_0^1 and 0_0^0 spectra recorded in the B^+A_4 channel are shown in Fig. 6(b). It is clear that the features to the blue of those assigned to the BA_3 cluster appear at the exact same frequencies in the B^+A_4 channel indicating that they represent absorption features of the BA_4 cluster. The most prominent features in the B^+A_4 channel at $-8.6/-7.5$, 8.2, 41.8/44.4, and 50.4/51.7 can be assigned to four geometrical isomers of the BA_4 cluster (BA_4-I, BA_4-II, BA_4-III, and BA_4-IV, respectively). The peaks to the red of the BA_4-I isomer (with a relatively strong feature at -31.8 cm^{-1}) appear in the B^+A_5 channel and therefore, are assigned to the BA_5 cluster or other higher clusters. Several weaker features are assigned to vdW modes associated with the isomers BA_4-I, BA_4-II, BA_4-III, and BA_4-IV. The two strongest isomers BA_4-III and BA_4-IV appear in the 0_0^0 spectrum [Fig. 6(b)] at 42 and 50 cm^{-1} with respect to the benzene origin. These peaks exhibit the expected 6_0^1 splitting as shown in Fig. 6(b) (top) and $0_0^0/6_0^1$ intensity ratios of about 8% and 6%, respectively. The relative frequencies and tentative assignments of the BA_3 and BA_4 features are listed in Table II. Figure 7 displays the overall R2PI spectra recorded in the benzene and the BA_n mass channels with $n=1-4$.

D. Spectral shifts

The spectral shifts relative to the 6_0^1 origin of the isolated benzene molecule imposed by acetonitrile clusters provide information on the nature of the intermolecular interactions within the binary clusters. A redshift is usually observed in clusters where the dispersion energy is the predominant interaction energy because of the increase in the molecular polarizability in the excited state relative to the ground state.[32,33] In the case of acetonitrile clusters, the binding energy is mainly due to electrostatic dipole–dipole interaction. Monte Carlo and molecular dynamics calculations have shown that the intermolecular interactions in small acetonitrile clusters ($n=2-9$) are dominated by configurations in which the molecular dipoles are aligned in an antiparallel fashion.[50,51] If the assumption is made that the presence of the benzene molecule will not significantly alter the favorable dipole–dipole interaction among the acetonitrile molecules, then the shift of the electronic origins of the BA_n clusters can be related to the interaction between the paired acetonitrile dipoles and the benzene ring.

The moderate blueshift observed for the BA cluster (37.6 cm^{-1}) is consistent with weak hydrogen bonding interaction between the CH_3 group of acetonitrile and the π-electron system of the benzene ring.[62] For example, benzene complexes with H_2O, CH_3OH, CH_3COOH, HCl, and $CHCl_3$ exhibit blueshifts of 52, 44, 152, 125, and 179 cm^{-1}, respectively.[21–26,30] It is interesting, however, to note that the addition of a second water (W) or methanol (M) molecule to the BW or to the BM complex results in a greater blueshift. For example, the spectral shifts of BW_2 and BM_2 clusters relative to the 6_0^1 origin of the isolated benzene molecule are 75 and 80 cm^{-1}, respectively.[23,24] On the other hand, the addition of a second acetonitrile molecule to the BA complex induces a red shift of -12 cm^{-1} relative to the 38 cm^{-1} shift of the BA complex. The shift continues toward the red since the two isomers of the BA_3 cluster (BA_3-I and BA_3-II) exhibit origin shifts of 1.5 and -13.6 cm^{-1}, respectively. This trend seems to switch over in the BA_4 cluster where the four assigned isomers BA_4-I, BA_4-II, BA_4-III, and BA_4-V display origin shifts of -8, 8.2, 41.8, and 50.4 cm^{-1}, respectively. This can be explained based on the evolution of the structures of these isomers. Based on the structure of the acetonitrile dimer, the BA_2 cluster is expected to have two antiparallel (head-to-tail) acetonitrile molecules placed above the benzene ring. This structure maximizes the dipole–dipole interaction between the two acetonitrile molecules and results in optimum interaction between the paired dipoles and the benzene ring. The differential redshift upon the addition of the second acetonitrile molecule is attributed to the weakening of the hydrogen-bonded interaction between the me-

TABLE III. Fragmentation probabilities of the BA_n cluster ions.

Fragmentation channel	Parent, shift (cm^{-1})	% 6_0^1	% 0_0^0
$BA^+ \rightarrow B^+$	BA (37.6)	31	17
$BA_2^+ \rightarrow BA^+$	BA_2 (25.9/27.2)	10.6	8.8
$\rightarrow B^+$	BA_2 (25.9/27.2)	35	21
$BA_3^+ \rightarrow BA_2^+$	BA_3 isomer I (−13.8/12.6)	42	36
$\rightarrow BA_2^+$	BA_3 isomer II (1.4/4.2)	48/41	28/20
$BA_4^+ \rightarrow BA_3^+$	BA_4 isomer III (41.8/44.4)	36	
$\rightarrow B^+$	BA_4 isomer III (41.8/44.4)	50	
$\rightarrow BA_3^+$	BA_4 isomer IV (50.4/51.7)	25	
$\rightarrow BA_2^+$	BA_4 isomer IV (50.4/51.7)	16	
$\rightarrow B^+$	BA_4 isomer IV (50.4/51.7)	45	

thyl group of acetonitrile and the benzene ring as a result of maximizing the favorable dipole pairing with the second acetonitrile molecule. Unlike the case of water or methanol, the second acetonitrile molecule is incapable of forming a strong hydrogen bond with the acetonitrile molecule attached to the benzene ring. It appears that the energy gain by the alignment of the acetonitrile dipoles in an antiparrallel configuration above the benzene ring is more than that resulting from the interaction of a second acetonitrile molecule with the weakly hydrogen bonded BA complex. The pairing of the acetonitrile dipoles in the BA_2 cluster requires changes in the B:A interaction which results in weakening of the hydrogen bonding between the methyl hydrogens and the benzene ring.

The increased redshift of the BA_3-II isomer may reflect a geometry where the acetonitrile trimer forms a cyclic structure above the benzene ring. This structure is expected to enhance the dispersion interaction, which typically results in red spectral shifts.[32,33] The possibility of having four isomers of the BA_4 cluster with different spectral shifts suggests that the structures of these isomers may involve different combinations of hydrogen bonding and dipole pairing interactions. It is interesting to note that isomer BA_4-IV exhibits a blue shift that is nearly twice the shift of the BA_2 cluster. This may suggest that the BA_4-IV isomer consists of two pairs of acetonitrile molecules, one pair on each side of the benzene ring. The MC minimum energy structures of the BA_n clusters will be presented and discussed in Sec. IV F.

E. Fragmentation of the ionized clusters

The excitation of the benzene's $A_{1g} \rightarrow B_{2u}$ 6_0^1 resonance in BA_n clusters by one-color R2PI (259.00 nm) deposits excess energy of at least 0.35 eV in the resulting cluster ion depending on the ionization energy of the cluster. The ionic state of the benzene molecule in the BA_n cluster is prepared according to the Franck–Condon distribution, while the rest of the cluster relaxes structurally in a time-dependent manner about the benzene ion. Because this relaxation releases energy, the actual cluster ionization threshold is lower than that of the isolated benzene molecule, and the additional energy is imparted to the cluster ion B^+A_n, thus promoting fragmentation via solvent evaporation from the cluster.

Fragmentation probabilities are measured by comparing the absolute integrated intensities I_n at various mass channels (parent I_n and daughters I_{n-1}, I_{n-2}, etc.) at the laser wavelength of a specific spectral resonance and normalizing to the sum over $I_n + I_{n-1} + \cdots$, etc. The results expressed as a percent of the parent ion intensity are shown in Table III. Within the two photon's energy limit, 31% and 17% of the B^+A complex fragment into the benzene mass channel (B^+) upon photoionization via the 6_0^1 and the 0_0^0 resonance excitations, respectively. The relatively efficient fragmentation observed for the B^+A complex following photoionization is a direct consequence to the π-hydrogen bonded geometry in the neutral complex. The structural change from the π-hydrogen bonding in the neutral species to the predominantly ion-dipole interaction in the ionized species involves a great strain, which leads to efficient fragmentation. However, the fragmentation of the B^+A complex is much less than that of the B^+W or B^+M complexes, where almost 100% fragmentations were observed. This is consistent with the assumption that the hydrogen-bonding interaction via the methyl group of acetonitrile to the benzene ring is much weaker than that between water or methanol with benzene.

The major fragmentation route of the B^+A_2 cluster is the loss of acetonitrile dimer (35% and 21% via the 6_0^1 and the 0_0^0 excitations, respectively) through the apparent $B^+A_2 \rightarrow B^+$ process. However, it should be pointed out that based on the densities-of-states of the species involved, RRKM calculations would predict that the most portable and fastest path for such process is $B^+A_2 \rightarrow B^+A \rightarrow B^+$. Since the ionization energy of the clusters goes down, the added excess energy in the cluster causes further continued fragmentation. As a result of the fast continuous evaporation, the overall $B^+A_2 \rightarrow B^+A \rightarrow B^+$ process has higher probabilities than the single $B^+A_2 \rightarrow B^+A$ process where the measured probabilities via the 6_0^1 excitation are 35% and 10.6%, respectively. The trend of increasing fragmentation as the cluster size increases continues for the BA_3 cluster where the $B^+A_3 \rightarrow B^+A_2$ channel exhibits 42% and 48% fragmentation probabilities via the 6_0^1 resonance of the two isomers, respectively. The two strongest isomers of the BA_4 cluster show significant fragmentations down to the B^+ channel. The loss of four acetonitrile molecules can be considered as sequential evaporation of single acetonitrile molecules from the B^+A_4 cluster. It is interesting to note that the BA_4-IV isomer shows sequential fragmentations into the B^+A_3, B^+A_2, and B^+

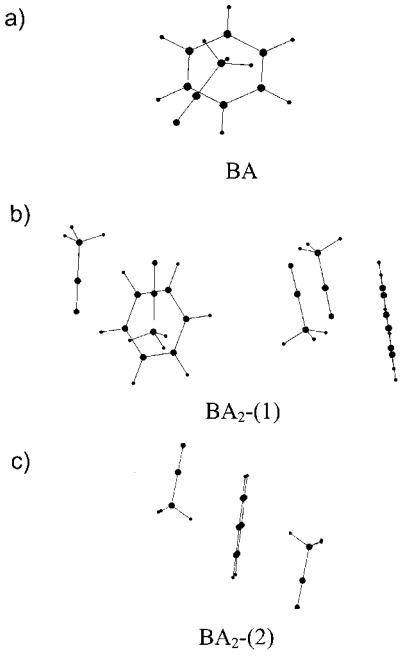

FIG. 8. Monte Carlo optimized structures of the BA and BA_2 clusters.

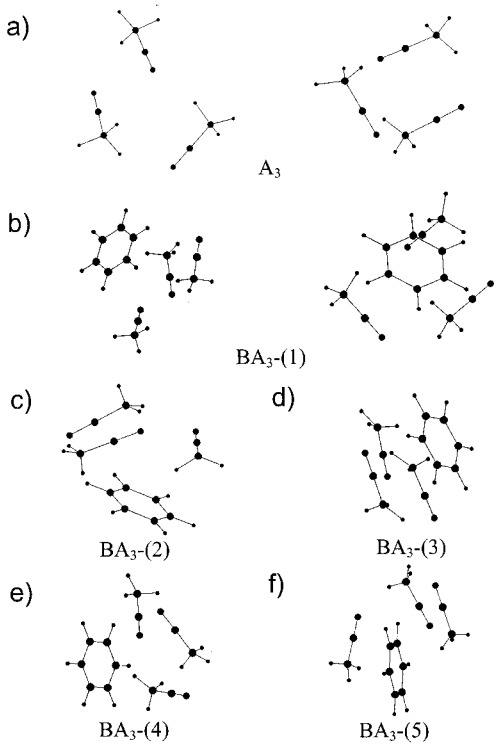

FIG. 9. Monte Carlo optimized structures of the A_3 cluster and the five lowest energy structures of the BA_3 cluster.

mass channels (25%, 16%, and 45%, respectively), while the BA_4-III isomer fragments only to the B^+A_3 and B^+ mass channels (36% and 50%, respectively). The dynamics of evaporation may be influenced by the specific arrangements of acetonitrile molecules with respect to the benzene ring. However, the present experiments do not provide direct information on the dynamics of solvent evaporation. It will be interesting to study the evaporation processes in the neutral clusters. For example, the evaporation of dimers from acetonitrile clusters has been suggested to explain the anomalous slow nucleation rates of supersaturated acetonitrile vapors as compared to the rates predicted by the classical theory of nucleation.[47–49]

F. Structures of isomers

1. Benzene (acetonitrile) and benzene (acetonitrile)$_2$

The MC structure for the BA complex obtained by the quenching procedure described in Sec. III is shown in Fig. 8(a). The acetonitrile molecule sits above the benzene ring with the methyl group close to, but not exactly above, the ring center. The distance between the center-of-mass of the benzene and acetonitrile molecules is 3.79 Å. The total interaction energy calculated according to the site–site potentials of Eq. (1) (Bohm 6-site potential for acetonitrile and Jorgensen OPLS 12-site potential for benzene) is -3.70 kcal/mol, with the Coulomb energy accounting for 58% of this interaction energy. This structure reproduces most of the major features of the *ab initio* fully optimized structure at the HF-6-31G** level.[62]

The equilibrium structure of the BA_2 cluster [BA_2-(1)] is shown in Fig. 8(b). In this structure, the two acetonitrile molecules exhibit a structure very similar to the equilibrium structure of the acetonitrile dimer calculated in the absence of the benzene molecule. The total interaction energy of the BA_2-(1) structure is -10.0 kcal/mol with the contribution from the interaction between the two acetonitrile molecules as -5.6 kcal/mol. This latter value is similar to the interaction energy (-5.7 kcal/mol) obtained upon removal of the benzene from the BA_2-(1) structure followed by relaxation of the remaining A_2 structure. This indicates that the presence of the benzene molecule does not significantly alter the structure of the acetonitrile dimer. This reflects the stronger dipole–dipole interaction in the acetonitrile dimer as compared to the weaker dipole-induced dipole interaction between acetonitrile and benzene.

The BA_2 structure where each acetonitrile molecule lies at opposite sides of the benzene ring [BA_2-(2) shown in Fig. 8(c)] has a much higher energy (-7.6 kcal/mol) than the BA_2-(1) structure (-10.0 kcal/mol). It should be noted that the BA_2-(2) structure is not compatible with the spectral shift of 26/27 cm^{-1} observed for the BA_2 cluster. Based on the additive role of spectral shifts, one would expect a shift of 52/54 cm^{-1} for the BA_2-(2) structure. Therefore, the lowest energy BA_2-(1) structure is assigned to the BA_2 cluster and is consistent with the observed spectral shift.

2. Benzene (acetonitrile)$_3$

Using the MC quenching technique, ten structures were found within a 10% energy range of the lowest energy isomer of the BA_3 cluster (-16.4 to -14.9 kcal/mol). The five lowest energy isomers along with the structure of the A_3 cluster are shown in Fig. 9; and the interaction energies are listed in Table IV. The lowest energy isomer BA_3-(1) consists of an acetonitrile trimer in a $2+1$ (dimer+monomer) ''T'' shape structure placed on the same side of the benzene

TABLE IV. Total interaction energies (E_{total}) of the Monte Carlo structures of the $C_6H_6(CH_3CN)_n$ clusters calculated using the OPLS potential (Ref. 57) for benzene (12-site) and the Bohm potential (Ref. 58) for acetonitrile (6-site).

Structure	Cluster	$-E_{total}$, kcal/mol
BA	$C_6H_6(CH_3CN)$	3.70
A_2	$(CH_3CN)_2$	5.65
BA_2-(1)	$C_6H_6(CH_3CN)_2$	9.99
BA_2-(2)		7.62
A_3	$(CH_3CN)_3$	10.80
BA_3-(1)	$C_6H_6(CH_3CN)_3$	16.37
BA_3-(2)		16.17
BA_3-(3)		15.84
BA_3-(4)		15.76
BA_3-(5)		15.50
A_4	$(CH_3CN)_4$	19.43
BA_4-(1)	$C_6H_6(CH_3CN)_4$	24.59
BA_4-(2)		24.52
BA_4-(3)		23.82
BA_4-(4)		23.74
BA_4-(5)		23.68
BA_4-(6)		23.64
BA_5-(1)	$C_6H_6(CH_3CN)_5$	30.98
BA_5-(2)		30.74
BA_5-(3)		30.60
BA_5-(4)		30.39
BA_5-(5)		30.34
BA_5-(6)		30.25
BA_6-(1)	$C_6H_6(CH_3CN)_6$	39.46
BA_6-(2)		39.38
BA_6-(3)		39.09
BA_6-(4)		38.84
BA_6-(5)		38.80
BA_6-(6)		38.72

ring. The A_2 pair of the A_3 trimer is the nearest to the benzene ring. The structure of the acetonitrile trimer is almost unchanged in the presence or absence of the benzene ring. For example, the total interaction energy of the BA_3-(1) structure is -16.4 kcal/mol with the contribution from the interaction among the acetonitrile trimer as -10.7 kcal/mol. This energy component is similar to the interaction energy obtained upon removal of the benzene from the BA_3-(1) structure followed by relaxation of the remaining A_3 structure (-10.8 kcal/mol). The BA_3-(2) isomer is very similar to the BA_3-(1) structure (A_3 exists in a $2+1$ configuration) except that the unpaired acetonitrile molecule is now the nearest to the benzene ring. The BA_3-(3) isomer represents an alternating head to tail configuration among the three acetonitrile molecules in a non planar structure above the benzene ring. In the BA_3-(4) isomer the three acetonitrile molecules form more of a cyclic structure than a $2+1$ ''T'' shape structure. The BA_3-(5) isomer, unlike all others, shows that the three acetonitrile molecules are all antiparallel and wrap around the benzene ring. The ''upper'' and ''lower'' acetonitrile molecules both attach to the benzene ring much as in the BA structure.

The observed spectral shifts of the BA_3 cluster were assigned to two isomers of the cluster, BA_3-I and BA_3-II. Both structures BA_3-(1) and BA_3-(4) are compatible with the redshifted BA_3-I isomer ($-12.6/-13.8$ cm^{-1}) where the dispersion interaction is expected to dominate the interaction energy in these structures. Structure BA_3-(5) is assigned to the second isomer BA_3-II that exhibits a very small blueshift (2/4 cm^{-1}). This structure allows for the sequential addition of a fourth acetonitrile molecule to the other side on the benzene ring thus, forming a BA_4 structure with one acetonitrile dimer on each side of the benzene ring.

3. Benzene (acetonitrile)$_4$

Fourteen structures were found within a 10% energy range of the lowest energy isomer of the BA_4 cluster (-24.6 to -22.0 kcal/mol). The six lowest energy isomers along with the structure of the A_4 cluster are shown in Fig. 10; and the interaction energies are listed in Table IV. The structure of the acetonitrile tetramer consists of two antiparallel pairs at right angles to each other with total interaction energy of -19.43 kcal/mol. The presence of the benzene ring does not alter the structure of the acetonitrile tetramer as shown in Fig. 10(b), where the lowest energy isomer of the BA_4 cluster, BA_4-(1), retains the structures of the two A pairs. It is also clear that although all the A molecules are on the same side of the benzene ring, only one of the two pairs is attached to the ring. The next isomer, BA_4-(2), has also two A pairs at right angles to each other, but the benzene ring has attachment to both pairs. The BA_4-(3) isomer still has all of the A molecules on the same side of the benzene, but one of the A molecules now reaches the plane of the benzene. Isomer BA_4-(4) presents an interesting structure where the four A molecules are nearly coaxial, and the plane of benzene is roughly perpendicular to the axes of the A molecules. The four A molecules form a rectangular quartet and all nearest neighbors are antiparallel, but those diagonally across from one another are parallel. In the next isomer BA_4-(5), the A molecules start to wrap around the benzene ring with an antiparallel pair+A on one side of the benzene and a single A on the other side. This structure can be formed by the addition of one A molecule to the BA_3-(5) structure, which was assigned to the BA_3 isomer that exhibits a small blue shift (2/4 cm^{-1}). The addition of one acetonitrile molecule to the other side of the benzene ring in structure BA_3-(5) is expected to induce a blue shift similar to that of the BA complex (38 cm^{-1}). Using the additive role, one expects the resulting BA_4-(5) structure to exhibit a blue shift of 40/42 cm^{-1}. It is interesting to note that one of the four isomers assigned to the BA_4 cluster (isomer BA_4-III) exhibits a blueshift of 42/44 cm^{-1} and therefore, structure BA_4-(5) is assigned to the BA_4-III isomer. The next BA_4 isomer [BA_4-(6)], consist of two A pairs, one above and the other below the plane of the benzene ring. Based on the additive role, one expects isomer BA_4-(6) to exhibit twice the blue shift of the BA_2 cluster (26/26 cm^{-1}). Interestingly, isomer BA_4-IV shows a blue shift of 50/52 cm^{-1}, and therefore, structure BA_4-(6) is assigned to the BA_4-IV isomer.

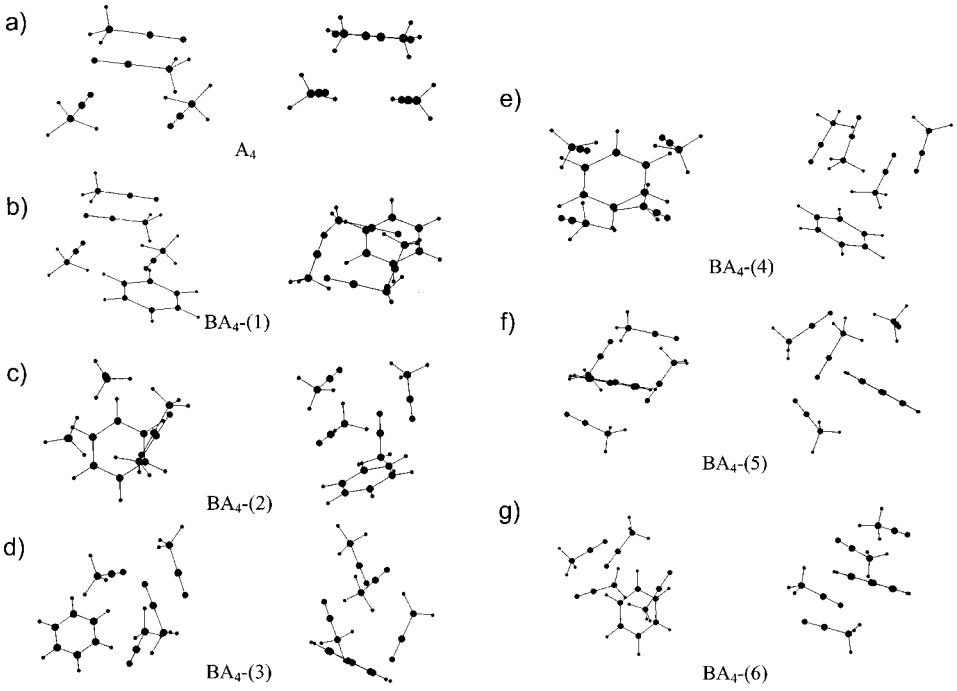

FIG. 10. Monte Carlo structures of the A_4 cluster and the six lowest energy structures of the BA_4 cluster.

4. Larger clusters, benzene (acetonitrile)$_5$ and benzene (acetonitrile)$_6$

Figures 11 and 12 display the six lowest energy structures of the BA_5 and BA_6 clusters, respectively, and the corresponding interaction energies are listed in Table IV. Most of the structures of the BA_5 isomers are irregular with no symmetry features especially in comparison to the neighboring BA_4 isomers. In all the isomers found for the BA_5 cluster, the acetonitrile molecules wrap around the benzene and do not lie on one side of the benzene ring. Isomer BA_5-(1) consists of one A pair and a head-to-tail arrangement of the remaining three A molecules. Isomer BA_5-(2) has very similar structure except the three A molecules tend to form a cyclic structure on one side of the benzene ring. Isomer BA_5-(3) consists of two A pairs, one on each side of the ring and the fifth A molecule in the plane of benzene. The formation of a cyclic structure from three A molecules appears again in isomer BA_5-(4) with the remaining A pair on the other side of the benzene ring, very similar to isomer BA_5-(2). Isomers BA_5-(5) and BA_5-(6) represent two A pairs, one on each side of the ring and the fifth A molecule in or perpendicular to the plane of the benzene ring. It is interesting to note that one of the A pairs in the BA_5-(6) isomer forms an up–down–up structure with the fifth A molecule. This structure wraps around the benzene and joins an antiparallel A pair on the other side of the ring. In general, the isomers obtained for the BA_5 cluster can be classified to three structural classes. The first class represents head-to-tail-type of interaction among the A molecules which wrap around the benzene ring [isomer BA_5-(1)]. The second class consists of two A pairs with the fifth A molecule within the benzene plane [isomers BA_5-(3), BA_5-(5), and BA_5-(6)]. The final class consists of a cyclic A trimer on one side of the benzene and an A pair on the other side [isomers BA_5-(2) and BA_5-(4)].

The structures obtained for the BA_6 cluster are very different from those of the BA_5 cluster. All the isomer found for the BA_6 cluster show that all the A molecules are clearly on the same side of the benzene ring. The pairing of A molecules is almost always clear in all the isomers as shown in Fig. 12. These isomers differ mostly in the way the three A pairs arrange themselves and how the benzene ring is attached. For example, isomers BA_6-(1) and BA_6-(2) represent three stacked A pairs in alternating perpendicular orientations. Isomers BA_6-(3) and BA_6-(4) show that two of the

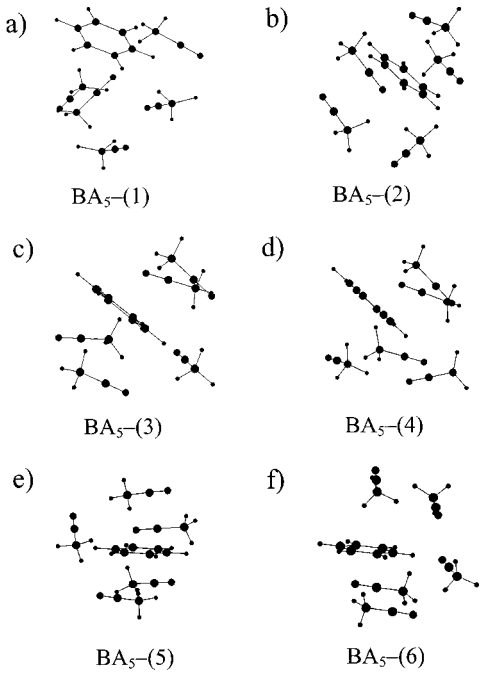

FIG. 11. Monte Carlo structures of the six lowest energy structures of the BA_5 cluster.

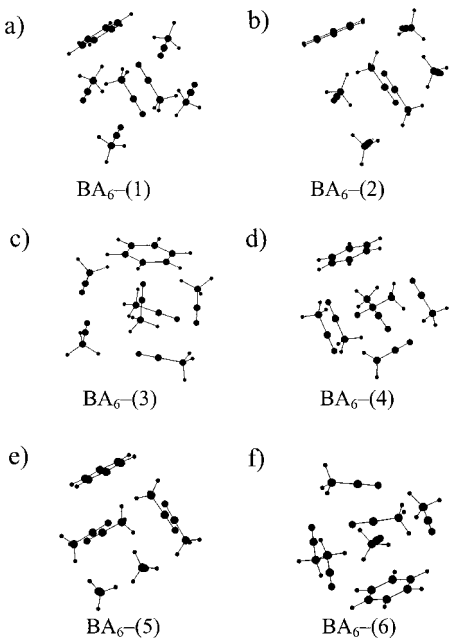

FIG. 12. Monte Carlo structures of the six lowest energy structures of the BA_6 cluster.

A pairs are formed by antiparallel orientations between two molecules in opposite planes. All the BA_6 isomers confirm the tendency for A molecules to exist in antiparallel and displaced parallel dimers even in the presence of the benzene molecule. This is much more effective for clusters containing even number of acetonitrile molecules. For example, for BA_4 and BA_6 clusters most of the isomers show clear pairing of the acetonitrile molecules into dimers.

V. SUMMARY AND CONCLUSIONS

In the present work, well-resolved spectra of benzene-acetonitrile binary clusters BA_n, with $n=1-4$ have been obtained by the (one-color) resonant two-photon ionization technique using benzene's $B_{2u}\leftarrow A_{1g}$ 0_0^0 and 6_0^1 spectral resonances. The spectra reveal a rapid increase in complexity with the number of acetonitrile molecules in the cluster, associated with van der Waal modes and isomeric forms. While only single cluster origins are found for the BA and the BA_2 clusters, two and four distinct isomers are identified for the BA_3 and BA_4 clusters, respectively. The origins of the BA and BA_2 clusters are blueshifted with respect to the free benzene molecule by 38 and 26 cm^{-1}, respectively. The blueshift is rationalized in terms of the weak hydrogen bonding interaction between the methyl group of acetonitrile and the benzene π-cloud. The photoionized BA_n clusters exhibit significantly smaller fragmentation probabilities compared to typical hydrogen bonding systems such as benzene $(water)_n$ and benzene $(methanol)_n$ clusters. The tendency for acetonitrile molecules to exist in antiparallel and displaced parallel dimers is clearly visible even in the presence of the benzene molecule. This is much more effective for clusters containing even number of acetonitrile molecules. Monte Carlo simulations reveal two types of isomeric structures of the BA_n clusters. The clusters containing an even number of the acetonitrile molecules (BA_2, BA_4, and BA_6) are dominated by acetonitrile anti-parallel paired dimers. The BA_3 cluster consists of a cyclic acetonitrile trimer in parallel configuration to the benzene ring. In the BA_5 clusters, the acetonitrile molecules are assembled in a cyclic trimer+a paired dimer structure, or in two paired dimers+a single monomer configuration. The R2PI spectra, in conjunction with the MC structural models and simple energetic arguments, provide a reasonably compelling picture of the spectroscopic and dynamical phenomena associated with dipole pairing molecular cluster systems.

ACKNOWLEDGMENT

The authors gratefully acknowledge financial support from the NSF Grant No. CHE 9816536.

[1] A. J. Stone, *The Theory of Intermolecular Forces* (Clarendon, Oxford, 1996).
[2] J. N. Israelachvili, *Intermolecular and Surface Forces* (Academic, London, 1997).
[3] J. A. Jeffrey, *Introduction to Hydrogen Bonding* (University Press, Oxford, 1997).
[4] *Molecular Interactions: From van der Waals to Strongly Bound Complexes*, edited by S. Scheiner (Wiley, New York, 1997).
[5] *Structure and Dynamics of Weakly Bound Complexes*, edited by A. Weber (NATO-ASI, Washington, D.C., 1988).
[6] E. R. Bernstein, in *Atomic and Molecular Clusters*, edited by E. R. Bernstein (Elsevier, Amsterdam, 1990).
[7] Q. Y. Shang and E. R. Bernstein, Chem. Rev. **94**, 2015 (1994).
[8] A. W. Castleman, Jr. and S. Wei, Annu. Rev. Phys. Chem. **45**, 685 (1994).
[9] T. S. Zwier, Annu. Rev. Phys. Chem. **47**, 205 (1996).
[10] A. W. Castleman, Jr. and K. Bowen, Jr., J. Phys. Chem. **100**, 12911 (1996).
[11] K. H. Fung, H. L. Selzle, and E. W. Schlag, J. Phys. Chem. **87**, 5113 (1983).
[12] K. S. Law, M. Schauer, and E. R. Bernstein, J. Chem. Phys. **81**, 4871 (1984).
[13] M. Schauer and E. R. Bernstein, J. Chem. Phys. **82**, 3722 (1985).
[14] K. O. Bornsen, H. L. Selzle, and E. W. Schlag, J. Chem. Phys. **85**, 1726 (1986).
[15] J. Wanna, J. A. Menapace, and E. R. Bernstein, J. Chem. Phys. **85**, 1795 (1986).
[16] J. B. Hopkins, D. E. Powers, and R. E. Smalley, J. Phys. Chem. **85**, 3739 (1981).
[17] P. R. R. Langridge-Smith, D. V. Brumbaugh, C. A. Haynam, and D. H. Levy, J. Phys. Chem. **85**, 3742 (1981).
[18] D. C. Easter, M. S. El-Shall, M. Y. Hahn, and R. L. Whetten, Chem. Phys. Lett. **157**, 277 (1989).
[19] X. Li, M. Y. Hahn, M. S. El-Shall, and R. L. Whetten, J. Phys. Chem. **95**, 8524 (1991).
[20] B. F. Henson, G. V. Hartland, V. A. Venturo, R. A. Hertz, and P. M. Felker, Chem. Phys. Lett. **176**, 91 (1991).
[21] A. J. Gotch and T. S. Zwier, J. Chem. Phys. **93**, 6977 (1990).
[22] J. R. Gord, A. W. Garrett, R. E. Bandy, and T. S. Zwier, Chem. Phys. Lett. **171**, 443 (1990).
[23] A. J. Gotch, A. W. Garrett, D. L. Severance, and T. S. Zwier, Chem. Phys. Lett. **178**, 121 (1991).
[24] A. J. Gotch and T. S. Zwier, J. Chem. Phys. **96**, 3388 (1991).
[25] A. J. Gotch, A. W. Garrett, and T. S. Zwier, J. Phys. Chem. **95**, 9699 (1991).
[26] A. W. Garrett, D. L. Severance, and T. S. Zwier, J. Chem. Phys. **96**, 7245 (1992).
[27] J. A. Menapace and E. R. Bernstein, J. Phys. Chem. **91**, 2843 (1987).
[28] P. M. Maxton, M. W. Schaeffer, and P. M. Felker, Chem. Phys. Lett. **241**, 603 (1995).
[29] P. Hobza, H. L. Selzle, and E. W. Schlag, Chem. Rev. **94**, 1767 (1994).
[30] I. N. Germanenko and M. S. El-Shall, J. Phys. Chem. **103**, 5847 (1999).
[31] G. M. Daly, D. Wright, and M. S. El-Shall, Chem. Phys. Lett. **331**, 47 (2000).
[32] H. C. Longuet-Higgins and J. A. Pople, J. Chem. Phys. **27**, 192 (1957).

[33] E. Shalev, N. Ben-Horin, and J. Jortner, J. Chem. Phys. **94**, 7757 (1991); E. Shalev, N. Ben-Horin, U. Even, and J. Jortner, *ibid.* **95**, 3147 (1991).
[34] R. N. Pribble and T. S. Zwier, Science **265**, 75 (1994).
[35] K. Kim, K. D. Jordan, and T. S. Zwier, J. Am. Chem. Soc. **116**, 11568 (1994).
[36] R. N. Pribble, A. W. Garrett, K. Haber, and T. S. Zwier, J. Chem. Phys. **103**, 531 (1995).
[37] S. Y. Fredericks, K. D. Jordan, and T. S. Zwier, J. Phys. Chem. **100**, 7810 (1996).
[38] C. J. Gruenloh, J. R. Carney, C. A. Arrington, T. S. Zwier, S. Y. Fredericks, and K. D. Jordan, Science **276**, 1678 (1997).
[39] C. J. Gruenloh, J. R. Carney, F. C. Hagemeister, C. A. Arrington, T. S. Zwier, S. Y. Fredericks, J. T. Wood III, and K. D. Jordan, J. Chem. Phys. **109**, 6601 (1998).
[40] J. R. Carmey, F. C. Hagemeister, and T. S. Zwier, J. Chem. Phys. **108**, 3379 (1998).
[41] P. Tarakeshwar, H. S. Choi, S. J. Lee, K. S. Kim, T. Ha, J. H. Jang, J. G. Lee, and H. Lee, J. Chem. Phys. **111**, 5838 (1999).
[42] R. D. Green, *Hydrogen Bonding by CH Groups* (Wiley, New York 1974).
[43] A. S. Al-Mubarak, G. Del Mistro, P. G. Lethbridge, N. Y. Abdul-Sattar, and A. J. Stace, Faraday Discuss. Chem. Soc. **86**, 209 (1988).
[44] U. Buck, X. J. Gu, R. Krohne, and Ch. Lauenstein, Chem. Phys. Lett. **174**, 247 (1990).
[45] U. Buck, Ber. Bunsenges. Phys. Chem. **96**, 1275 (1992).
[46] E. Knozinger, P. Beichert, J. Hermelling, and O. Schrems, J. Phys. Chem. **97**, 1324 (1993).
[47] D. Wright, R. Caldwell, and M. S. El-Shall, Chem. Phys. Lett. **176**, 46 (1991).
[48] D. Wright, R. Caldwell, C. Moxely, and M. S. El-Shall, J. Chem. Phys. **98**, 3356 (1993).
[49] D. Wright and M. S. El-Shall, J. Chem. Phys. **98**, 3369 (1993).
[50] G. Del Mistro and A. J. Stace, J. Chem. Phys. **99**, 4656 (1993).
[51] D. Wright and M. S. El-Shall, J. Chem. Phys. **100**, 3791 (1994).
[52] H. B. Lavender, K. A. Iyer, and S. J. Singer, J. Chem. Phys. **101**, 7856 (1994).
[53] V. Molinero, D. Laria, and R. Kapral, J. Chem. Phys. **109**, 6844 (1998).
[54] M. S. El-Shall and Z. Yu, J. Am. Chem. Soc. **118**, 13058 (1996).
[55] M. S. El-Shall, G. M. Daly, Z. Yu, and M. Meot-Ner, J. Am. Chem. Soc. **117**, 7744 (1995).
[56] W. L. Jorgensen and J. M. Briggs, Mol. Phys. **63**, 547 (1988).
[57] W. L. Jorgensen and D. L. Severance, J. Am. Chem. Soc. **112**, 4768 (1990).
[58] H. J. Bohm, I. R. McDonald, and P. A. Madden, Mol. Phys. **49**, 347 (1983).
[59] M. P. Allen and D. J. Tildesley, *Computer Simulation of Liquids* (Oxford University, Oxford, 1991).
[60] G. H. Atkinson and C. S. Parmenter, J. Mol. Spectrosc. **73**, 20 (1978); **73**, 31 (1978); **73**, 52 (1978).
[61] U. Boesl, J. Phys. Chem. **95**, 2949 (1991).
[62] G. M. Daly, C. Schultz, C. Castevens, D. D. Shillady, and M. S. El-Shall, in *Science and Technology of Atomically Engineered Materials*, edited by P. Jena, A. N. Khanna, and B. K. Rao (World Scientific, New Jersey, 1996), p. 251.
[63] F. Lahmani, A. Zehnacker-Rentein, and E. Breheret, J. Phys. Chem. **94**, 8767 (1990).
[64] V. Brenner, A. Zehancker, F. Lahmani, and Ph. Millie, J. Phys. Chem. **97**, 10570 (1993).